ISBN: 978-3-95450-227-1 ISSN: 2673-5490 doi:10.18429/JACoW-IPAC2022-THPOST016

DEVELOPMENT PROGRESS OF HEPS LINAC*

C. Meng†, N. Gan, D. Y. He, X. He, Y. Jiao, J. Y. Li, J.D. Liu, X.H. Lu, Y. M. Peng, X.J. Nie, H. Shi, G. Shu, S. C. Wang, O. Z. Xiao, J. R. Zhang, Z.D. Zhang, Z.S. Zhou
Key Laboratory of Particle Acceleration Physics and Technology,
Institute of High Energy Physics, 100049, Beijing, China

Abstract

The High Energy Photon Source (HEPS) is a synchrotron radiation source of ultrahigh brightness and under construction in China. Its accelerator system is comprised of a 6-GeV storage ring, a full energy booster, a 500-MeV Linac and three transfer lines. The Linac is an S-band normal conducting electron linear accelerator with available bunch charge up to 10 nC. The Linac online equipment installation and vacuum connection in the tunnel has been finished at May 2022. The system joint debugging and device conditioning of the accelerating units, the power supplies, et al., are in progress. The beam commissioning will start in August 2022. This paper presents the status of the HEPS Linac and detailed introduction of the beam commissioning simulations and preparations.

INTRODUCTION

The High Energy Photon Source (HEPS) [1] is a 4th generation synchrotron light source based on a 6 GeV diffraction-limited storage ring [2] that is current under construction in northern China. The injector consists of a 500-MeV Linac [3], a full-energy booster [4], a low energy transfer line connecting the Linac and booster and two transfer lines transferring beams back and forth between the storage ring and booster [5]. The Linac is a normal conduction S-band linear accelerator and main parameters are show in Table 1. The Linac is composed of three subsystems includes an electron gun, a bunching system and the main accelerator. A thermal cathode electron gun is adopted and can provide larger than 10 nC electron beam per pulse. The baseline scheme of bunch structure is one bunch per pulse. However, based on the consideration of retaining certain TMCI charge threshold margin of booster, the Linac could be configured to provide three-bunches-per-pulse beams. So, the bunching system [6] includes two sub-harmonic bunchers (SHB), one pre-buncher (PBUN), one buncher (BUN) and one accelerating structure (AS). In the main Linac, there are eight accelerating structures driven by four klystrons and five triplets. The Linac layout is shown in Fig.1.

Table 1: Main Parameters of The Linac

Parameter	Unit	Value
RF frequency	MHz	2998.8
Energy	MeV	500
Max. Repetition frequency	Hz	50
Pulse charge	nC	0.5~7
Number of bunches per pulse	-	1 or 3
Bunch length (rms)	ps	~5
Energy spread (rms)	%	≤0.5
Emittance (rms)	nm	70

* Work supported by the High Energy Photon Source (HEPS) project, a major national science and technology infrastructure project and the Youth Innovation Promotion Association CAS (2019016)
† mengc@ihep.ac.cn

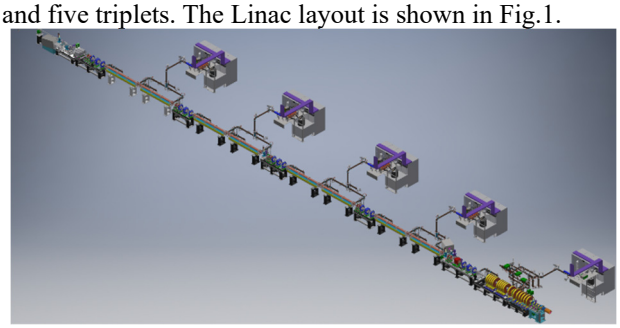

Figure 1: The layout of Linac.

The planed Linac beam commissioning will start in August this year. Before this, beam commissioning preparations should be completed. Now, the Linac equipment is being installed and vacuum connection in the tunnel has been finished. In this paper, beam commissioning simulation is presented in the second part and the status of Linac construction is presented at the third part.

BEAM COMMISSIONING SIMULATION

The main measured parameters of HEPS Linac are emittance, energy and energy spread. In order to suppress short longitudinal wakefield effect, the acceleration phase decreases as bunch charge increases. Phase scan method is adopted to obtain the offset between the physical phase and LLRF phase. In this part, the information of emittance measurement, energy and energy spread measurement, phase scan and orbit corrections are introduced. A new platform python accelerator physics application set (Pyapas) is under developing [7] to be used in the Linac beam commissioning and all the related commissioning applications based on Pyapas have been finished.

Emittance Measurement

The method used to measure the transverse emittance of beam is quadrupole scan [8] by measure the transverse beam size while changing the upstream quadruples. The beam size σ_i at measurement point location can express in matrix formulation by

$$\begin{pmatrix}\sigma_1^2\\ \sigma_2^2\\ \vdots\\ \sigma_n^2\end{pmatrix}_2 = \begin{pmatrix}R_{11} & R_{12} & R_{13}\\ R_{21} & R_{22} & R_{23}\\ \vdots & \vdots & \vdots\\ R_{n1} & R_{n2} & R_{n3}\end{pmatrix}\begin{pmatrix}\beta\varepsilon\\ \alpha\varepsilon\\ \gamma\varepsilon\end{pmatrix}_1 = \mathrm{R}\begin{pmatrix}\beta\varepsilon\\ \alpha\varepsilon\\ \gamma\varepsilon\end{pmatrix}_1 \quad (1)$$

$$\begin{aligned} R_{i1} &= m_{11}^2\\ R_{i2} &= -2m_{11}m_{12}\\ R_{i3} &= m_{12}^2 \end{aligned} \quad (2)$$

where "1" indicate the emittance measurement point and "2" indicate he beam size measurement point, and m_{ij} is

ISBN: 978-3-95450-227-1 ISSN: 2673-5490 doi:10.18429/JACoW-IPAC2022-THPOST016

the elements of transformation matrix. Then we can get the sigma matrix element by

$$\begin{pmatrix}\beta\varepsilon\\ \alpha\varepsilon\\ \gamma\varepsilon\end{pmatrix}_1 = (R^T R)^{-1} R^T \begin{pmatrix}\sigma_1^2\\ \sigma_2^2\\ \vdots\\ \sigma_n^2\end{pmatrix}_2 \quad (3)$$

and the emittance by

$$\varepsilon = \sqrt{\beta\varepsilon\cdot\gamma\varepsilon - (\alpha\varepsilon)^2}. \quad (4)$$

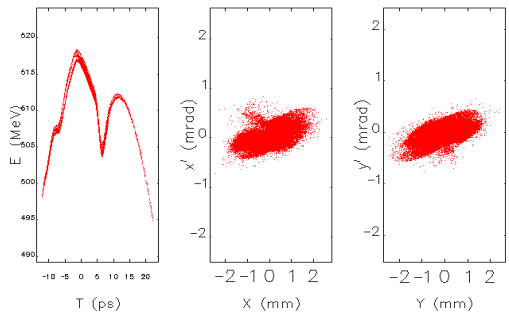

Figure 2: Beam distribution used in emittance measurement.

There are three profile monitors (PR) in the main Linac, where can measure the emittance with beam energy about 50 MeV, 280 MeV and 500 MeV. Using the PR, we can get the horizontal and vertical beam size simultaneously, so we change both the focusing and defocusing quadrupoles and measure the beam sizes, then the emittance can be calculated. Table 2 shows the simulation results at 510 MeV with different beam size measurement errors. The input beam distribution used in the simulation is shown in Fig.2. The beam size errors are uniform distribution with 1000 seeds. According to simulation results, the measured emittance uncertainly is about 10%.

Table 2: Emittance Measurement Simulation Results

Parameters	Unit	Reference	Error: 1% mean(std)	Error: ±0.1mm mean(std)
ε_x	nm	93.8	93.5(0.73)	93.8(5.6)
β_x	m	4.647	4.645(0.097)	4.655(0.442)
α_x		-0.552	-0.555(0.007)	-0.553(0.062)
ε_y	nm	81.5	81.1(1.5)	81.6(7.6)
β_y	m	5.016	5.024 (0.141)	5.048(0.603)
α_y		-0.687	-0.693(0.016)	-0.693(0.099)

Energy and Energy Spread Measurement

There are two energy analysis transport lines (EATLs) for measuring the beam energy and energy spread at low and high energies, respectively. We can get the beam energy by

$$E[\mathrm{MeV}] = \frac{299.79\cdot BL(I)[T\cdot m]}{\frac{\Delta x}{L}+\theta_0} \quad (5)$$

where θ_0 is designed angle of energy analysis transport line, L is the distance between the exit of analysis magnet and PR target, Δx is beam position, $BL(I)$ is the integral magnetic field and E is beam energy. The energy measurement accuracy is about 0.2% and analysis results are shown in Table3. The orbit is main factor affecting energy measurement accuracy.

Table 3: Energy Measurement Accuracy Analysis

Parameter	unit	Low energy analysis transport line		High energy analysis transport line	
		Value	Measurement accuracy	Value	Measurement accuracy
L	mm	631.5	/	1013	/
ρ	mm	670	/	2100	/
θ_0	mrad	436.33	/	200.00	/
Dispersion	mm	329.6	/	245.1	/
PR target misalignment	mm	0.15	5.4×10^{-4}	0.15	7.4×10^{-4}
PR target accuracy	mm	0.1	3.6×10^{-4}	0.1	4.9×10^{-4}
Orbit	mm	0.5	1.8×10^{-3}	0.3	1.5×10^{-3}
power supply accuracy	/	2.5×10^{-4}	3.5×10^{-4}	2.5×10^{-4}	3.5×10^{-4}
Magnetic field accuracy	/	5.0×10^{-4}	5.0×10^{-4}	5.0×10^{-4}	5.0×10^{-4}
Total	/	/	0.2%	/	0.18%

Table 4: Energy Spread Measurement Simulation Results

EATL	Ref. δ	Eq.(8)	Eq.(7)	Beam size error: ±1% mean (std)	Beam size error: ±5% mean (std)
Low	5.30%	5.43%	5.43%	5.43% (0.03%)	5.43% (0.16%)
High	0.844%	0.881%	0.868%	0.868% (0.01%)	0.868% (0.025%)

The beam size at PR target can express by

$$\sigma_{x,y} = \sqrt{\sigma_{\beta x,\beta y}^2 + \left(D_{x,y}\delta\right)^2}, \quad (6)$$

where $\sigma_{x,y}$ is measured beam size, $\sigma_{\beta x,\beta y}$ is the calculated beam size with Twiss parameters, $D_{x,y}$ is dispersion and δ is the momentum spread or energy spread. According to Eq.(6), we can get the energy spread as

$$\delta = \sqrt{\frac{\sigma_{x,y}^2-\sigma_{\beta x,\beta y}^2}{D_{x,y}^2}} \quad (7)$$

$$\delta = \sigma_{x,y}/D_{x,y}. \quad (8)$$

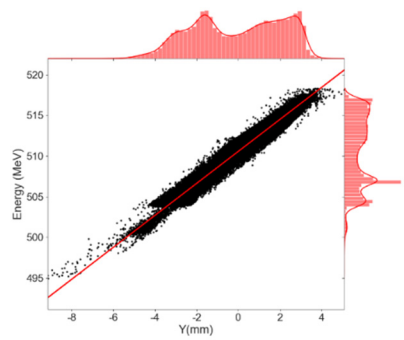

Figure 3: Phase space of y-E at High EATL PR target.

ISBN: 978-3-95450-227-1 ISSN: 2673-5490 doi:10.18429/JACoW-IPAC2022-THPOST016

In order to increase measurement resolution, we need a smaller β function at PR target. For simplicity, we can use Eq.(8) to calculate energy spread with small β function and big energy spread or at the beginning of commission stage when have not measure the twiss parameters. The energy spread measurement simulation results are shown in Table 4 and the phase space of *y*-*E* at High EATL PR target is shown in Fig.3.

Phase Scan

We use phase scan method to obtain the phase offset between physical accelerating phase and LLRF phase. With this value, we can set physical accelerating phase by LLRF. The energy can express by

$$E = E_0 + V_0 \cdot sin(\phi_s + \Delta\phi), \quad (9)$$

where E is measured energy at exit of accelerating structure, E_0, V_0 and ϕ_s is the input energy, accelerating voltage and LLRF phase of the accelerating structure, $\Delta\phi$ is the phase offset. While scanning the LLRF phase, we can measure the beam energy and fit the relationship between LLRF phase and energy by Eq. (9) to get the phase offset. We have simulated the measured accuracy with different number of measurements, different accelerating phase error and different energy measurement accuracy. The phase offset measurement accuracy (std value) is about 0.5 degree when number of measurements is 10, accelerating phase error is 0.3 degree and energy measurement accuracy is 0.2%. Because the orbit is different at different energy, the energy measurement accuracy is maybe larger and affects phase offset measurement accuracy greatly. We can iterate the measurement process by taking the orbit into consideration.

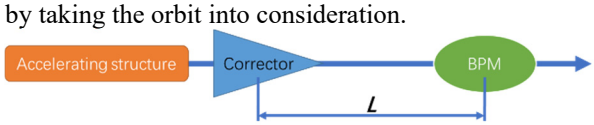

Figure 4: Phase scan schematic.

The beam with different energy passing through a corrector will have different kick angle and get different beam orbit at the following section. So, we can use one corrector and one BPM to measure the phase offset and the schematic is shown in Fig. 4. The measured orbit by BPM can express by

$$x = \left(\frac{1}{1+\frac{V_0}{E_0}\cdot sin(\phi_s+\Delta\phi)}\right) x_0, \quad (10)$$

where E_0 is the input energy, x_0 is the BPM reading with energy in E_0, $V_0$and ϕ_s is accelerating voltage and LLRF phase of the accelerating structure, x is the BPM readings. The initial x_0 can be set as 1~3mm. According to the simulation results, the phase offset measurement accuracy (std value) is about 0.5 degree when number of measurements is 30, accelerating phase error is 0.3 degree and BPM measurement accuracy is 50 μm. The second method only using BPM values is simple and can save measurement time.

Orbit Correction

When the bunch charge is large, the short transverse wakefield will greatly affect the beam orbit, so at the beginning of beam commissioning at high bunch charge mode, automate feedback based one-to-one correction scheme is adopted. The commissioning application of one-to-one correction scheme and global correction scheme have both been completed.

LINAC CONSTRUCTION STATUS

The first accelerating strucutre was transported into the Linac tunnel in March 8,2022, which represents the start of the in-tunnel installation. Until to May 12, 2022, the online equipment installation and vacuum connection in the tunnel has been finished and the photo is shown in Fig. 5. Before installation we have built three test platforms and completed high power testing of most high-power components, such as electron gun, klystron, accelerating structure, SHB, BUN, pulse compressor, load, and so on. The beam test of electron gun has been completed and results are shown in Fig. 6. The pulse charge can reach larger than 12 nC. The RF conditioning process of all the accelerating structures is shown in Fig. 7 and the calculated accelerating gradient is larger than 20 MV/m. Now the system joint debugging is in progress, and after that there is about one month for all system conditioning. The Linac beam commissioning will start in August 2022.

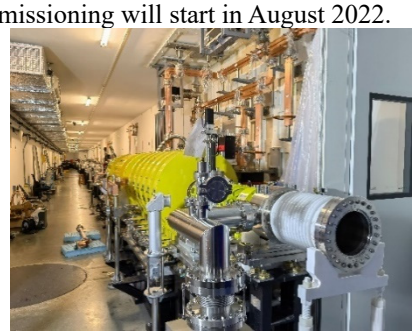

Figure 5: Photo of the Linac tunnel, May 12 2022.

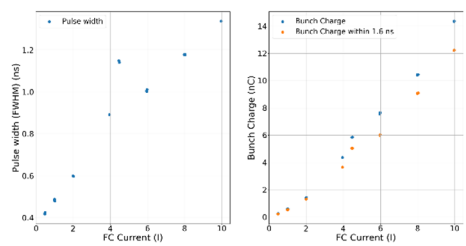

Figure 6: Beam test of electron gun.

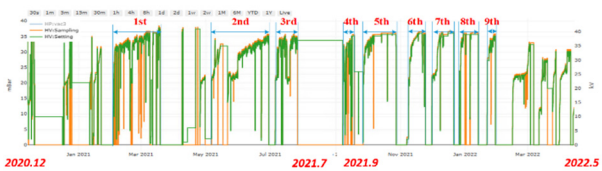

Figure 7: RF conditioning of nine accelerating structures.

CONCLUSION

The online equipment installation and vacuum connection of the HEPS Linac have been completed and the beam commissioning will start soon. Beam commissioning simulations are presented in this paper.

ISBN: 978-3-95450-227-1 ISSN: 2673-5490 doi:10.18429/JACoW-IPAC2022-THPOST016

REFERENCES

[1] Yi Jiao *et al*., "The HEPS project," *J. Synchrotron Rad.* (2018). 25, 1611-1618.

[2] Y. Jiao, F. Chen, P. He, *et al*., "Modification and optimization of the storage ring lattice of the High Energy Photon Source," *Radiat Detect Technol Methods* 4, 415–424 (2020).

[3] C. Meng, X. He, Y. Jiao *et al*., "Physics design of the HEPS LINAC," *Radiat Detect Technol Methods* 4, 497–506 (2020).

[4] Y. Peng, Z. Duan, Y. Guo *et al*., "Design of the HEPS booster lattice," *Radiat Detect Technol Methods* 4, 425–432 (2020).

[5] Y. Guo, Y. Wei, Y. Peng *et al*., "The transfer line design for the HEPS project," *Radiat Detect Technol Methods* 4, 440–447 (2020).

[6] S. Zhang, S. Wang, C. Meng *et al*., "The physics design of HEPS Linac bunching system," *Radiat Detect Technol Methods* 4, 433–439 (2020).

[7] X. H. Lu *et al*., "Status of High Level Application Development for HEPS", in *Proc. ICALEPCS'21*, Shanghai, China, Oct. 2021, pp. 978-980. doi:10.18429/JACoW-ICALEPCS2021-THPV047

[8] Helmut Wiedemann, "Particle Beams and Phase Space", in *Particle Accelerator Physics*, pp. 224-226, 2019.